Journal of Thermal Analysis, Vol. 46 (1996) 1775-1788

STRUCTURAL THERMAL AND TEXTURAL STUDIES ON COBALT OXIDE/ALUMINA SUPPORTED CATALYSTS

M. N. Ramsis, Ch. A. Philip, M. Abd El Khalik and E. R. Souaya

Department of Chemistry, Faculty of Science, Ain Shams University, Abbassia, Cairo, Egypt

(Received January 27, 1995; in revised form June 23, 1995)

Abstract

CoO/Al_2O_3 catalysts containing amounts of cobalt ranging form 2 to 20% were prepared at *pH* 11 from neutral mesoporous alumina composed of γ-Al_2O_3 and poorly crystalline boehmite, and were then dried at 80°C. X-ray diffraction, DTA and TG techniques were used to study the structural changes produced upon thermal treatment up to 700°C.

Soaking of the alumina in cobalt ammine complex solutions for a period of 10 days (the time required for equilibrium) resulted in a series of catalyst samples (I–V). Another sample (III-a) was soaked for a period of 5 days only in order to study the effect of the soaking time upon the equilibrium conditions.

Cobalt aluminate ($CoAl_2O_4$) bands were characterized in all catalyst samples except III-a. They increased in intensity with increasing cobalt content. Surface species appeared in samples heated to 80°C, and others persisted at 150°C. Heating to temperatures above 200°C resulted in the formation of cobalt oxides, due to decomposition of the surface compounds. DTA and TG studies showed that this was more pronounced at higher concentrations of cobalt. Samples heated at 500°C and above did not undergo any further structural changes, except that the boehmite in the support was converted to γ-Al_2O_3.

The variations in the surface parameters followed the same pattern as found previously [1], demonstrating that the catalyst samples are mesoporous, with retention of two ranges of pore size in most cases.

Keywords: catalysts, structural, thermal and textural characteristics

Introduction

The use of transition metals supported on silica or alumina as catalysts is well known [2–5]. The activity of catalysts is believed by some authors [6–8] to arise from a minimum size of ordered crystalline structure and from the dislocation density, and by others [9, 10] to arise from disordered parameters. All these factors depend on the initial preparative methods and subsequent thermal treatment. In previous work, nickel ammine complexes were supported on silica [11] and alumina [1]. The present work involves a parallel study of cobalt ammine complexes on alumina. A detailed thermal structural and textural study

0368–4466/96/ $ 5.00

John Wiley & Sons, Limited
Chichester

was carried out by means of techniques such as DTA, TG and XRD for thermal and structural studies, and N_2 adsorption for textural properties.

Experimental

The cobalt ammine complexes were prepared by dissolving varying amounts of $Co(NO_3)_2 \cdot 6H_2O$ (BDH grade) in water and adding NH_4OH solution with constant stirring until the precipitate formed just disappeared. Total volumes were adjusted to 225 ml. 30 g portions of alumina support were then soaked in the solutions with different concentrations of cobalt complexes and were allowed to stand at room temperature for 10 days with frequent stirring (samples I–V). Sample III-a was prepared by soaking for a period of 5 days only. Soaking was followed by filtration and drying overnight at 80°C.

After soaking, the *pH* dropped from ~11 to ~10. The cobalt content was estimated in solution before and after soaking by indirect complexometric titration [12]. Heat treatment was then applied to all samples in the temperature range 150–700°C for 2 h in static air.

The alumina was a product (neutral) used for chromatographic adsorption analysis (according to Brockman (II), Reanal, Hungary).

XRD patterns were obtained by using a Philips model pw 1050/70 X-ray diffractometer and iron-filtered cobalt radiation. The *d*-distances were calculated and their relative intensities compared with data in the ASTM cards [13, 14].

A Stanton-Redcroft 750/770 thermobalance connected to a Kipp and Zonnen BD9 two-channel automatic recorder was used for the TG analysis. The heating rate was 10°C min^{-1}.

DTA data were obtained with a Stanton-Redcroft STA 780 apparatus, using α-alumina as inert standard and a linear heating rate of 10°C min^{-1}.

A Pye-Unicam SP 3200 A spectrograph was used to obtain the IR spectra, with samples in KBr pellets.

A conventional volumetric apparatus was applied to determine the adsorption–desorption isotherms of purified nitrogen at 77 K.

Structural and thermal characteristics

X-ray

X-ray analysis of the alumina support showed that it was mainly composed of γ-alumina, together with a poorly crystalline boehmite and traces of K alumina. The intensity and crystallinity of the bands characterizing the support ($2\theta = 14.5$, 28.2 and 38.4) markedly increase on the penetration due to the presence of cobalt ions during a long soaking period (10 days) at high *pH*, as discussed previously [1]. We believe that the presence of cobalt ions is responsible for the crystallinity of boehmite and that the crystal geometry of the support is

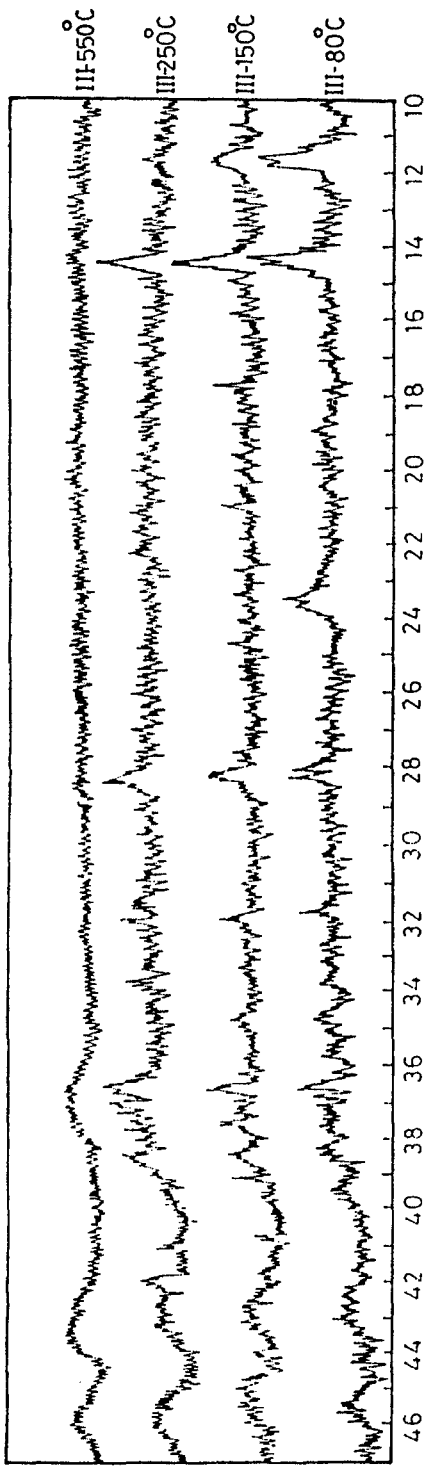

Fig. 1 XRD patterns of sample III and its thermally heated products

stabilized and improved when the cobalt ions penetrate and occupy the vacant cation sites.

The XRD patterns of all catalyst samples, with the exception of III-a, which represents non-equilibrium conditions, exhibit diffraction bands characteristic of $CoAl_2O_4$ ($2\theta = 36.6$ and 31.6) [13]. The intensities of these bands increased slightly with increasing cobalt content. The amphoteric alumina support could dissolve at *pH* 11 to give $[Al(OH)_4]^-(aq)$ or $[Al(H_2O)_2(OH)_4]^-$ [15], which in the presence of $[Co(NH_3)_5]^{2+}$ could form cobalt aluminate. It is possible considering the defect spinel structure of γ-Al_2O_3 and the related boehmite, it is possible that the alumina support supplies a suitable substrate for $CoAl_2O_4$ to form and grow on.

Thermal treatment affects the structural species markedly. Thus, the main band of $Co(OH)_2$ at $\theta = 37.8$ appears only for samples heated to 150°C. Heating at 250°C results in the appearance of cobalt oxide (2θ–42.5, 36.6 and 36.5) (Fig. 1). These bands increase in intensity with increasing cobalt concentration. At 550°C, the main peaks disappear. On heating to higher temperature, no further structural changes are observed.

A surface species appears in all samples heated to 80°C, with $2\theta =$ 23.0–28.2, even in sample III-a. On heating to 150°C, this band disappears completely (Fig. 1), probably because of the decomposition of this species, which may contain hydroxide ions and ammonia as ligands. This decomposition is also encountered in the TG study, as a loss in mass in this temperature range, as will be shown later in connection with the TG curves.

Besides these peaks, another one appears at 2θ–11.6 for all samples heated to 80°C, and it persists on heating to 150°C. For samples III and III-a, this band is split into three bands, two of which are shifted to lower 2θ values (10.3 and 9.7–9.9). Only these last two bands appear for sample IV heated to 150°C; they disappear completely for sample V (Fig. 2). Heating to higher temperatures causes the dissapearance of these bands from all catalyst samples. This is probably due to the formation of a complex species which starts to decompose during heating to form intermediate compounds which are completely transformed to cobalt oxide upon elevation of the temperature. This disappearance of these bands from sample V (with the highest content of cobalt) at 150°C, and their very low intensity at 80°C, may be due to the formation of this surface compound inside the pores. The high cobalt concentration facilitates its penetration inside the pores and, upon thermal treatment up to 250°C, ligands are evolved (molecular water from the hydroxo ligand and ammonia). This is also shown in the TG and DTG curves discussed later.

Thermogravimetric analysis

Figure 3 illustrates the TG curves of catalyst samples I–V and III-a. The curves display two overlapping steps, the first starting at about 50°C and terminating at ~125°C, followed immediately by another one terminating at 200°C.

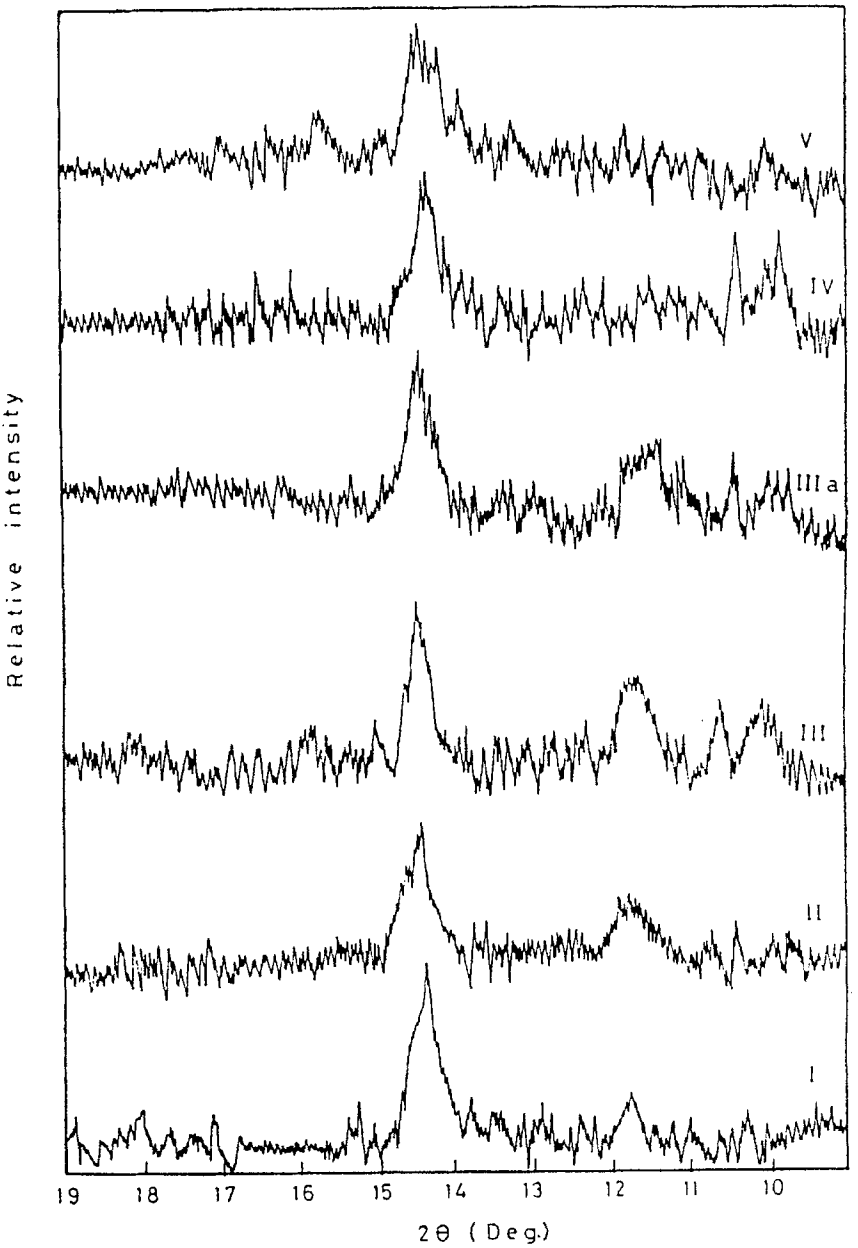

Fig. 2 XRD patterns of samples I–V and III-a heated at 150°C

Sample III-a shows only the first step. This loss in mass is probably due to the evolution of physically adsorbed water, which may be attached either to already adsorbed water molecules or to the surface hydroxy groups by H-bonding, and also to the evolution of physically adsorbed ammonia. The percentage mass loss

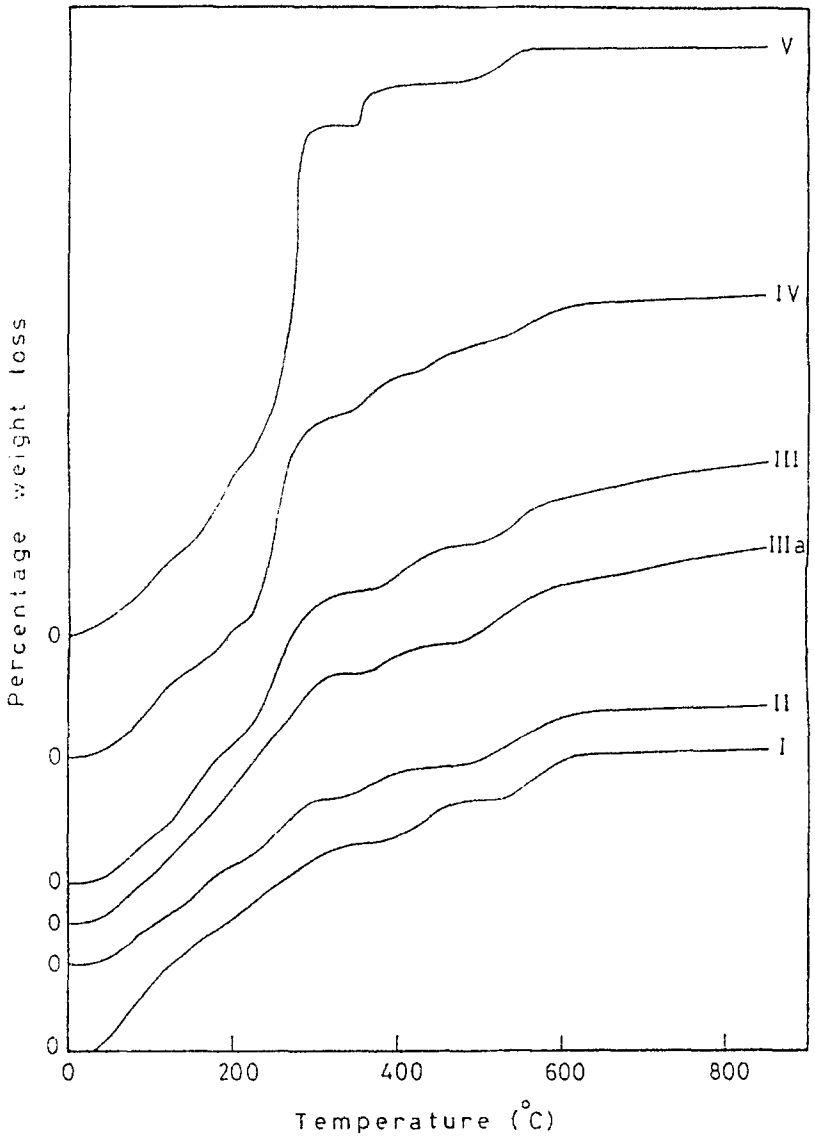

Fig. 3 Thermogravimetric curves for catalyst samples I–V and III-a

in the second step in Table 1 reveals an increase in mass loss with increasing cobalt content. This is plausible, since the presence of the ammonia ligand facilitates the further adsorption of water molecules (OH^- or H_2O) by H-bonding and the former is a function of the amount of cobalt present. The percentage mass loss observed in the range up to 125°C is constant for all samples except sample III-a, due to the equilibrium conditions.

Following these steps, a third one is observed, terminating at about 325°C, which is probably due to dehydration of the resulting $Co(OH)_2$ [16].

The percentage mass loss observed in this step depends strongly upon the cobalt content of the samples, as shown in Table 1, increasing with increasing cobalt concentration.

Table 1 Percentage weight loss for the investigated catalyst samples

Co content	Weight loss/%					
%CoO	1st step	2nd step	3rd step	4th step	5th step	Total loss
I	1.9	2.8	2.2	1.0	1.0	8.9
2.4						
II	1.9	2.5	1.5	0.7	1.2	7.8
6.3						
III	1.9	3.1	3.8	1.2	1.2	11.2
8.3						
IV	2.0	3.3	4.7	1.7	1.0	12.7
10.0						
V	2.1	4.0	8.0	8.0	1.1	23.0
13.8						
III-a	1.2	–	4.8	4.8	1.0	11.8
8.0						

A fourth step, starting at about 325°C and ending at about 500°C, then follows, and is found to consist of two steps for sample IV. In Fig. 4, which depicts the DTG curves of all samples (I–V), a main peak appears in the temperature range 200–300°C. For sample III, this peak is preceded by a shoulder, which is more pronounced in sample IV. As for sample V, with the highest Co concentration, only a sharp peak is observed. This step is believed to result from the decomposition of both the adsorbed species, which may be $[Co(NH_3)_5](NO_3)_2$ and $[Co(NH_3)_5](OH)_2$ or $[Co(NH_3)_6]^{3+}$, and the evolution of ammonia from the surface species, as discussed previously in the X-ray section. It was shown earlier that, in the case of sample V, the complex species is formed inside the pores and consequently will be less decomposed by heat. This is confirmed by the low percentage mass loss observed in comparison to the other samples with low cobalt content.

The fifth and last step occurs in the range 500–600°C, and is centered at 540°C in the DTG curves. It is unaffected by concentration and is due to boehmite dehydroxylation.

Sample III-a, soaked for 5 days only, demonstrates that the equilibrium conditions are not reached within this soaking period. This is obvious from the fact that, although the total percentage mass loss is slightly higher, the percentage

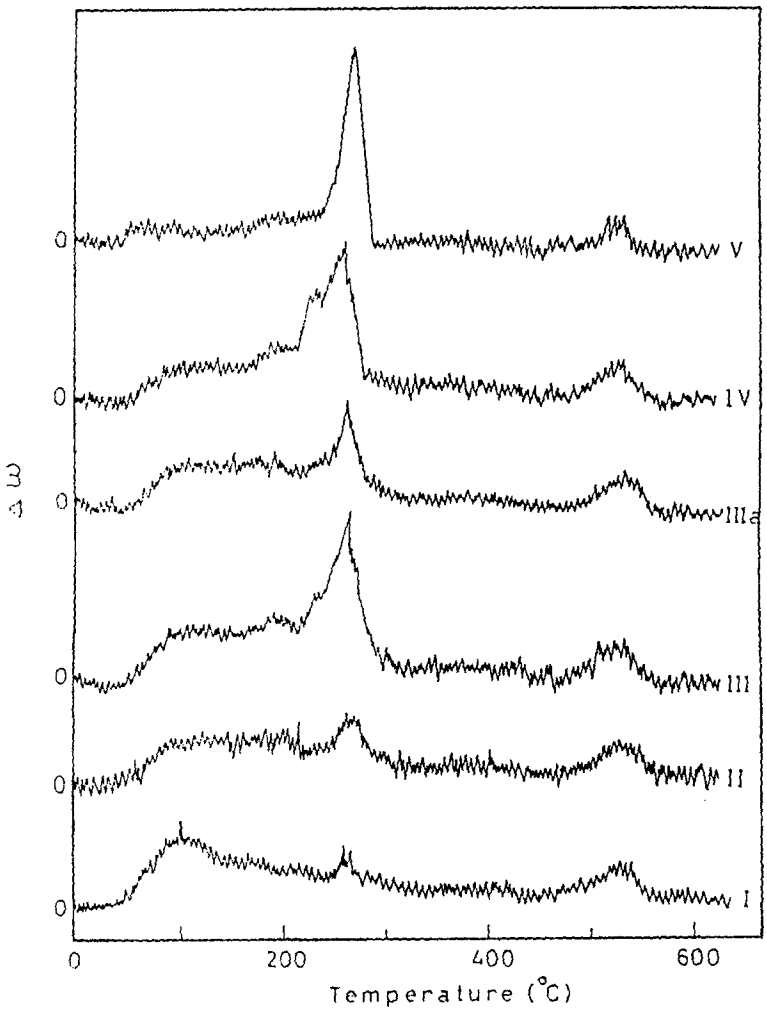

Fig. 4 Differential thermogravimetric analysis curves of catalyst samples I–V and III-a

mass loss for the third step is high as compared to the corresponding sample III with comparable cobalt content.

Differential thermal analysis

Upon heating, the ammine complexes adsorbed on alumina, which were originally pink (cobalt pentammine complexes), changed to blue, i.e. to mixed oxides [$CoO{\cdot}Co_2O_3$] [17].

The DTA curves of all catalyst samples (Fig. 5) display an endothermic peak in the temperature range 100–200°C. This broad endotherm arises from the evo-

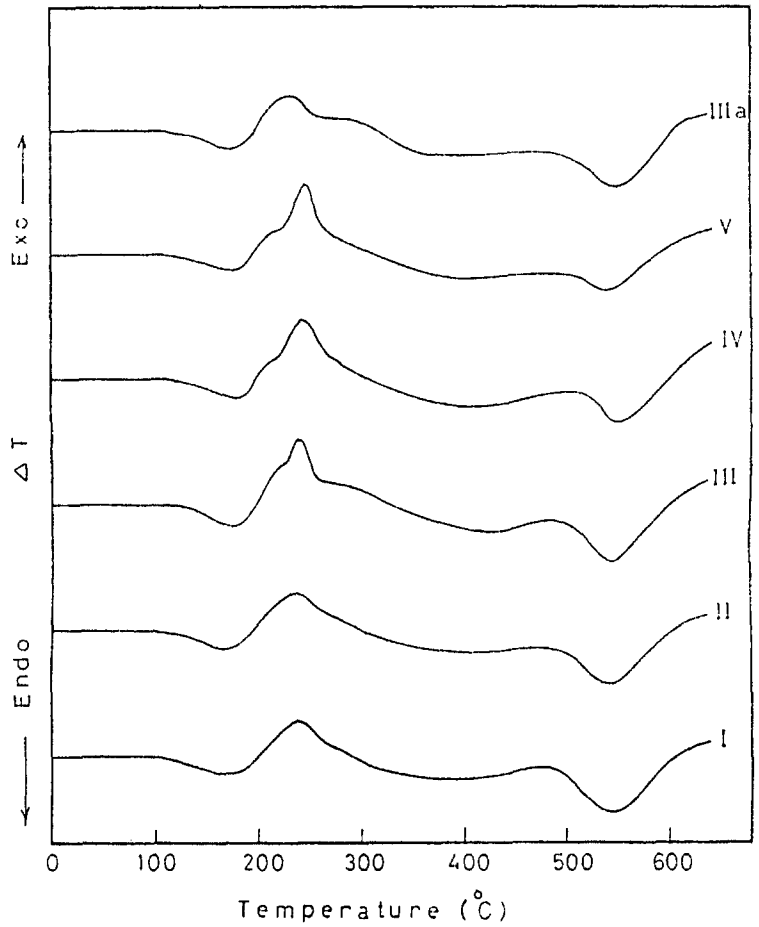

Fig. 5 Differential thermal analysis curves of catalyst samples I–V and III-a

lution of physically adsorbed (H-bonded) ammonia [18, 19] and water, as observed from the TG curves (Fig. 3).

The peak is directly followed by an exotherm centered at 240°C. This main peak is always followed by a shoulder, as shown by the arrow, sometimes preceded by another one, as in samples III, IV and V. This exotherm is probably due to decomposition of the surface adsorbed complex species and evolution of the ammonia ligand, which was found to be exothermic when the counterion was NO_3^- [20].

The endotherm interrupting the broad exotherm and appearing as a shoulder in the temperature ranges 200–220°C and 260–280°C is probably due to the evolution of chemisorbed ammonia. The two phenomena occur (Fig. 4) at the same time and only the net effect appears as shown in the DTG curves, where the two peaks are observed in the temperature region 200–300°C.

The endothermic plateau which follows probably results from evolution of the remaining chemisorbed ammonia (Fig. 5).

The last endotherm, centered at 540°C, results from the dehydroxylation of boehmite to γ-Al_2O_3 which is in accordance with the constant last mass loss in the TG curves.

Infrared

A broad band appears at about 3340 cm^{-1} in the spectra of all samples heated from 80 to 700°C and is attributed to the lattice water present in the alumina support. The band at 1060 cm^{-1} (some of the nitrate may be present in the coordination sphere as unidentate nitrate) disappears from the samples heated above 150°C.

Chemisorbed ammonia is still present at 700°C, as seen from the bands characterizing NH_3: δs (HNH) at 1370 cm^{-1}, and δa (HNH) at 1630 cm^{-1} [16]. They are shifted to higher frequencies, since they represent non-coordinated ammonia. This is in accordance with the DTA curves, which show the presence of such chemisorbed NH_3 as a plateau extending to 500°C, but interrupted by the stronger exothermic dehydroxylation of the alumina surface.

Textural characteristics

Effects of concentration and temperature

The adsorption–desorption isotherms of nitrogen at −196°C are obtained for all the catalyst samples and also for the thermally heated products of sample III. All isotherms are of type II of Brunauer's classification and exhibit hysterisis loops closed in the relative pressure range 0.45 to 0.6. The isotherms are much more rounded at the low-pressure end, and correspondingly the intercept on the $P/x(P^o-P)$ axis is farther away from the origin in the BET plot. The modifications observed for the surface texture were further predicted by a pore analysis, using the *t*-method [21, 22]. The analysis facilitated detection and differentiation between the micropores and the mesopores of the sample. In these plots, the *t*-curve of Mikhail *et al.* [23] for a non-porous solid with a low BET constant C which matched those of the samples being tested was used. S_t and S_{BET} agreed for all samples, thereby fulfilling the main criteria [24] for the correct choice of the *t*-curves used in the analysis. A typical set of V_1 *vs.* plots were constructed from the nitrogen-adsorption data for samples heated at 80°C or at 550°C, and a complete set of samples III and III-a and their thermally heated products are presented in Figs 6 and 7.

The samples are generally characterized by a relatively small BET constant C, the magnitude of which is considered to be an indication of the degree of interaction between the solid surface and the adsorbed layer. The specific surface

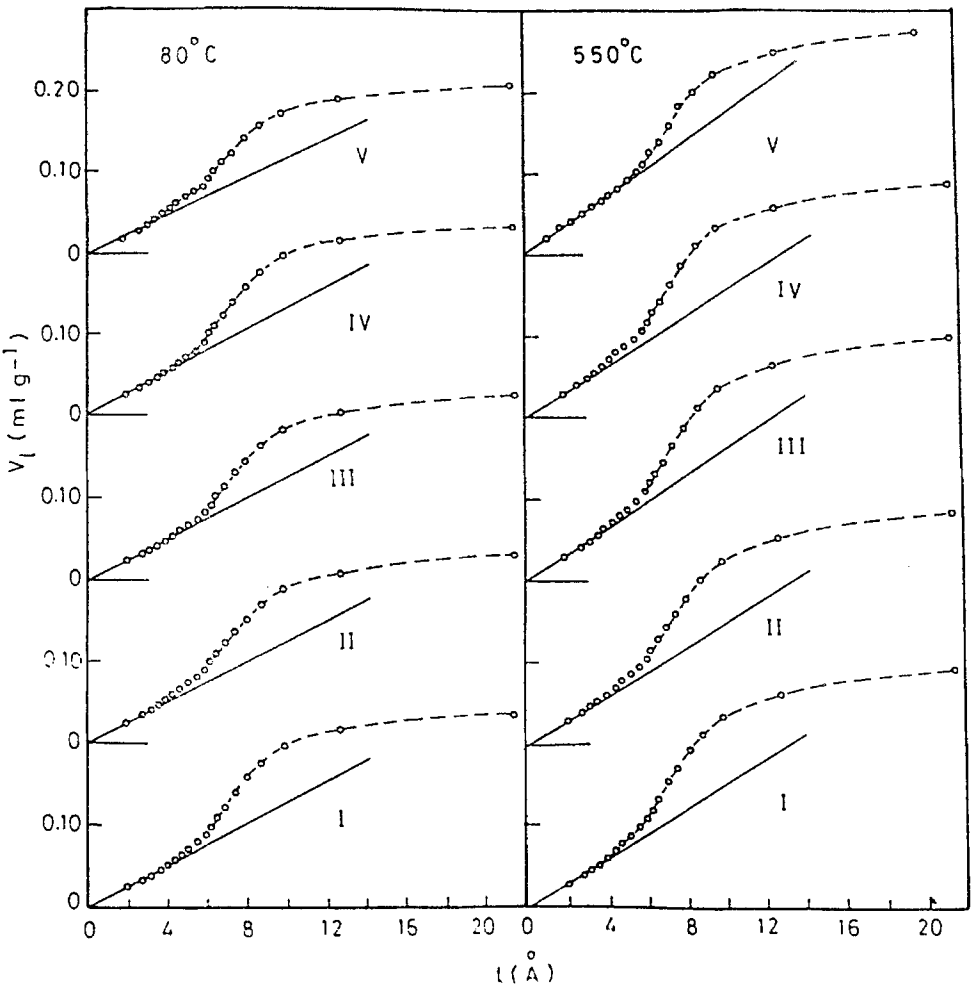

Fig. 6 V_l–t plots from nitrogen adsorption on catalyst samples I–V and their corresponding heated products at 550°C

areas (S_{BET}) were estimated by using the BET equation over its normal range of applicability and by adopting a value of 16.2 Å^2 for the cross-sectional area of the N_2 molecule.

On comparison of the original samples with the pure parent Al_2O_3 [1], it was observed that the presence of a small amount of cobalt caused a slight increase in the area, accompanied by a mild increase in the total pore volume and a corresponding decrease in the average pore radius (assuming parallel plates) (Table 2, columns 3–6). The changes observed in the crystallinity of boehmite upon impregnation in the cobalt ammine complex seem to be responsible for the resulting textural variation, since alterations in the crystallite dimensions are normally reflected in the pore system.

For sample II, the catalyst exhibits decreases in the area and total pore volume, and a slight increase in the average pore radius is observed; this is well reflected in the V_l *vs.* t plot, showing this small widening of the pores below t=0.6 nm. A further increase in cobalt content (sample IV) results in no noteworthy changes. S_{BET} and V_P 0.95 are slightly increased, with a corresponding narrowing of the pore size, as observed in the V_l *vs.* t plot (Fig. 6). Sample V was found to be much more influenced, with marked decreases in area and total pore volume. This occurred as a result of blocking of some of the pores creating two ranges of pore sizes in the mesoporous range: the first of narrowing dimensions, observed at t=4.4–6 Å, followed by a second group of wide pores at higher t.

The heating of sample III to 150°C causes some increase in the area and total pore volume, accompanied by a drastic decrease in the average pore radius rela-

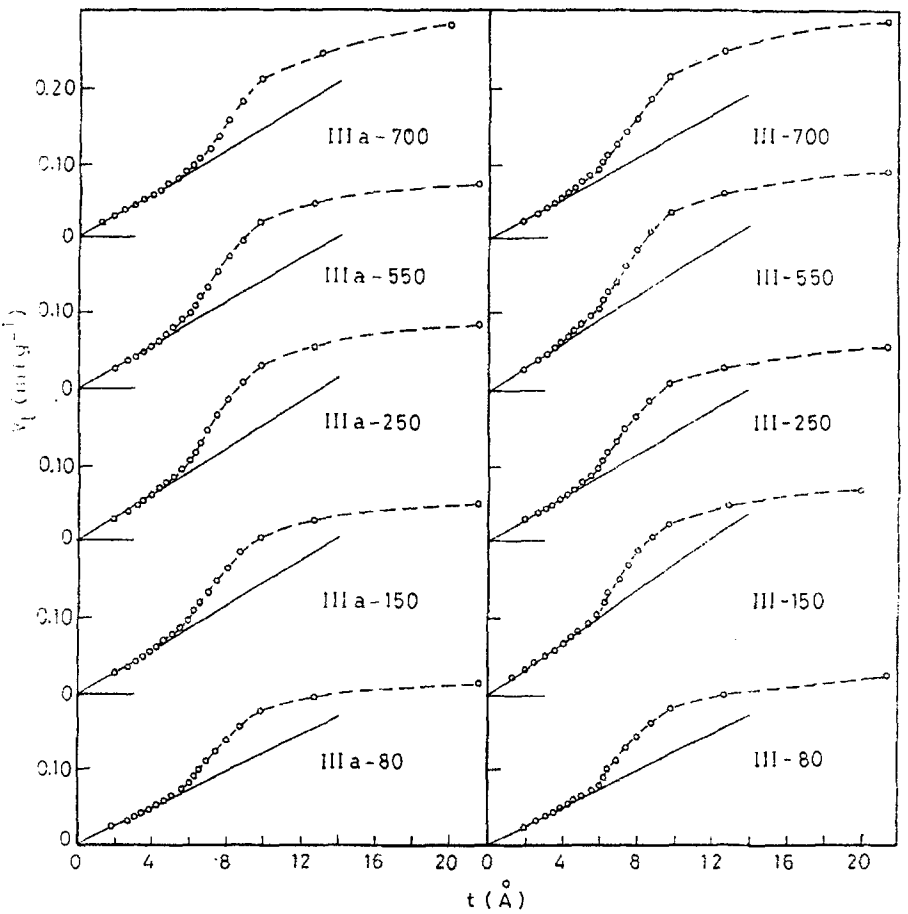

Fig. 7 V_l–t plots from nitrogen adsorption on catalyst samples III and III-a and their thermally treated products

tive to that of the original soaked sample. This may be due to the evolution of both physically adsorbed water and ammonia, together with the formation of new surface species, as discussed earlier. The slight decrease in the slope of the V_l *vs.* t plot revealed this mild change in the dimensions of the pore (Fig. 7). Increase of the temperature to 250°C decreases the area again, and also the total pore volume, but a sharp increase in the average pore radius (1.6 Å to 1.9 Å) is reflected by the upward deviation beginning at t=5 Å, P/P^o=0.4. The surface compound formed upon heat treatment at 150°C (see section XRD) and vanishing at higher temperature leads to a process analogous to the agglomeration of the particles creating new pore dimensions. All the catalyst samples display an obvious increase in surface area upon heat treatment at 550°C, accompanied by an increase in total pore volume and eventually a decrease in average pore radius (except for samples III and IV) (Table 2, Columns 3, 5 and 6). The full decomposition of ammines at this temperature and the evolution of chemisorbed NH_3 exposes new surface, which is additive to the support. The V_l *vs.* t plot for sample V at 550°C shows that up to t=6 Å we have a straight line passing through the origin, and the mesoporous character is reflected where an upward deviation commences t=6.2 Å, P/P^o=0.55.

Table 2 Surface parameters of catalyst samples I–V and their thermally heated products

Samples		BET C-constant	S_{BET}/ m^2g^{-1}	S_t/ m^2g^{-1}	$V_{p\,0.95}$/ ml g–1	r_h/ Å
I.	80°C	24	126.5	128	0.2480	1.91
II.	80°C	30	122.0	124	0.2356	1.93
III.	80°C	18	124.5	125	0.2262	1.82
IV.	80°C	19	129.1	130	0.2356	1.82
V.	80°C	20	112.0	115	0.2067	1.85
I.	550°C	19	155.6	154	0.2886	1.85
II.	550°C	19	147.2	148	0.2808	1.91
III.	550°C	16	159.9	158	0.2933	1.83
IV.	550°C	19	147.2	150	0.2824	1.92
V.	550°C	11	161.4	165	0.2675	1.66
III.	150°C	11	168.3	170	0.2714	1.61
III.	250°C	25	134.9	137	0.2358	1.90
III.	550°C	16	159.9	158	0.2933	1.83
III.	700°C	16	141.0	139	0.2863	2.03
Al_2O_3		30	120.0	121	0.2350	1.96
Al_2O_3 (Soaked in NH_4OH)		25	124.7	126	0.2700	2.16

The delay in the upward deviation relative to that for the original sample V may be interpreted as a result of a compensating effect [25] stemming from the presence of narrow pores (supermicropores) filled by multilayer formation and causing a downward deviation that opposes the corresponding upward deviation expected from the mesopores (of limited size) in the region of the plot.

Increase of the temperature to 700°C causes some shrinkage of the solid/void matrix, and hence a drop in the surface area, accompanied by a sharp increase in the average pore radius. This is an opportunity for capillary condensation to occur still at this temperature.

References

1 M. N. Ramsis, E. R. Souaya, M. Abd El Khalik and Suzy A. Selim, J. Mater. Sci., 25 (1990) 6.
2 J. R. Andersen, Sructure of Metallic Catalyst, Academic London, London 1975; Ch. 1.
3 J. Coyns, M. T. Chenebauc, J. F. Le Page and R. Montarnal, Preparation of Catalyst, B. Delmon, P. A. Jacobs and G. Poncelet (Eds). Elsevier, Amsterdam 1976.
4 J. Cervelle, G. Hermana, J. F. Jimenez and F. Melo, Preparation of Catalyst, B. Delmon, P. A. Jacobs and G. Poncelet (ed.). Elsevier, Amsterdam 1976.
5 M. Houalla, Stud. Surf. Sci. Catal., 16 (1983) 273.
6 G. Rienacker, Abh. Dtsch. Akad. Wis. Berlin, Kl. Chem. Geol. Biol., 3 (1956) 8.
7 H. Taylor, Adv. Catal., 9 (1957) 1.
8 P. Desai and J. T. Richardson, Catalyst Deactivation, B. Delmon, G. F. Froment (Eds.), Elsevier, Amsterdam 1980.
9 J. Bagg, H. Jaeger and J. V. Sanders, J. Catalog., 2 (1963) 449.
10 J. Uhara, T. Hikino, Y. Numata, H. Hamada and Y. Kageyama, J. Phys. Chem., 66 (1962) 1374.
11 Said Hanafi, Anwar Amin, Sara M. Oliman and Suzy A. Selim, Thermochim. Acta, 95 (1985) 159.
12 R. Pribil, Applied Complexometry, Pergamon Press, London 1982.
13 J. V. Smith (Ed.) 'X-ray Powder Data File and Index to X-ray Data File' American Society for testing and materials, Philadelphia, 1961.
14 Powder Diffraction File, ASTM Alphabetic Index of Inorganic Compounds, published by the International Center for Diffraction Data, 1978, SW Athmore, 19081, USA.
15 B. C. Lippens and J. J. Steggenta, 'Physical and Chemical Aspects of the Adsorbents and Catalysts', ed. by B. G. Linsen.
16 J. J. B. Van Voortuysen, E. Van and P. Franzen, Recl. Trav. Chim. Pays Bas., 70 (1951) 793.
17 N. N. Greenwood and A. Earnshaw, 'Chemistry of the Elements', Pergamon Press, London 1984.
18 N. W. Cant and L. M. Little, Can. J. Chem., 42 (1964) 802.
19 M. Folman and D. J. C. Yaes, Proc. R. Soc. London, Ser. A, 246 (1958) 32.
20 W. W. Wendlant and J. P. Smith, J. Inorg. Nucl. Chem., 26 (1964) 445.
21 B. C. Lippens, B. G. Linsen and J. H. De Boer, J. Catal., 3 (1964) 32.
22 J. H. De Boer, B. G. Linsen and Jh. J. Osinge, ibid 4 (1965) 643.
23 R. Sh. Mikhail, N. M. Guindy and S. Hanafi, Egypt. J. Chem., Special Issue 'Tourky' 53 (1973).
24 R. Sh. Mikhail and F. Shebl, J. Colloid Interface Sci., 34 (1970) 65.
25 R. Sh. Mikhail, J. Chem, UAR, 6 (1963) 26.